Immunity, Volume *45*

Supplemental Information

Transcriptional Landscape of Human Tissue Lymphocytes Unveils Uniqueness of Tumor-Infiltrating T Regulatory Cells

Marco De Simone, Alberto Arrigoni, Grazisa Rossetti, Paola Gruarin, Valeria Ranzani, Claudia Politano, Raoul J.P. Bonnal, Elena Provasi, Maria Lucia Sarnicola, Ilaria Panzeri, Monica Moro, Mariacristina Crosti, Saveria Mazzara, Valentina Vaira, Silvano Bosari, Alessandro Palleschi, Luigi Santambrogio, Giorgio Bovo, Nicola Zucchini, Mauro Totis, Luca Gianotti, Giancarlo Cesana, Roberto A. Perego, Nirvana Maroni, Andrea Pisani Ceretti, Enrico Opocher, Raffaele De Francesco, Jens Geginat, Hendrik G. Stunnenberg, Sergio Abrignani, and Massimiliano Pagani

Figure S1

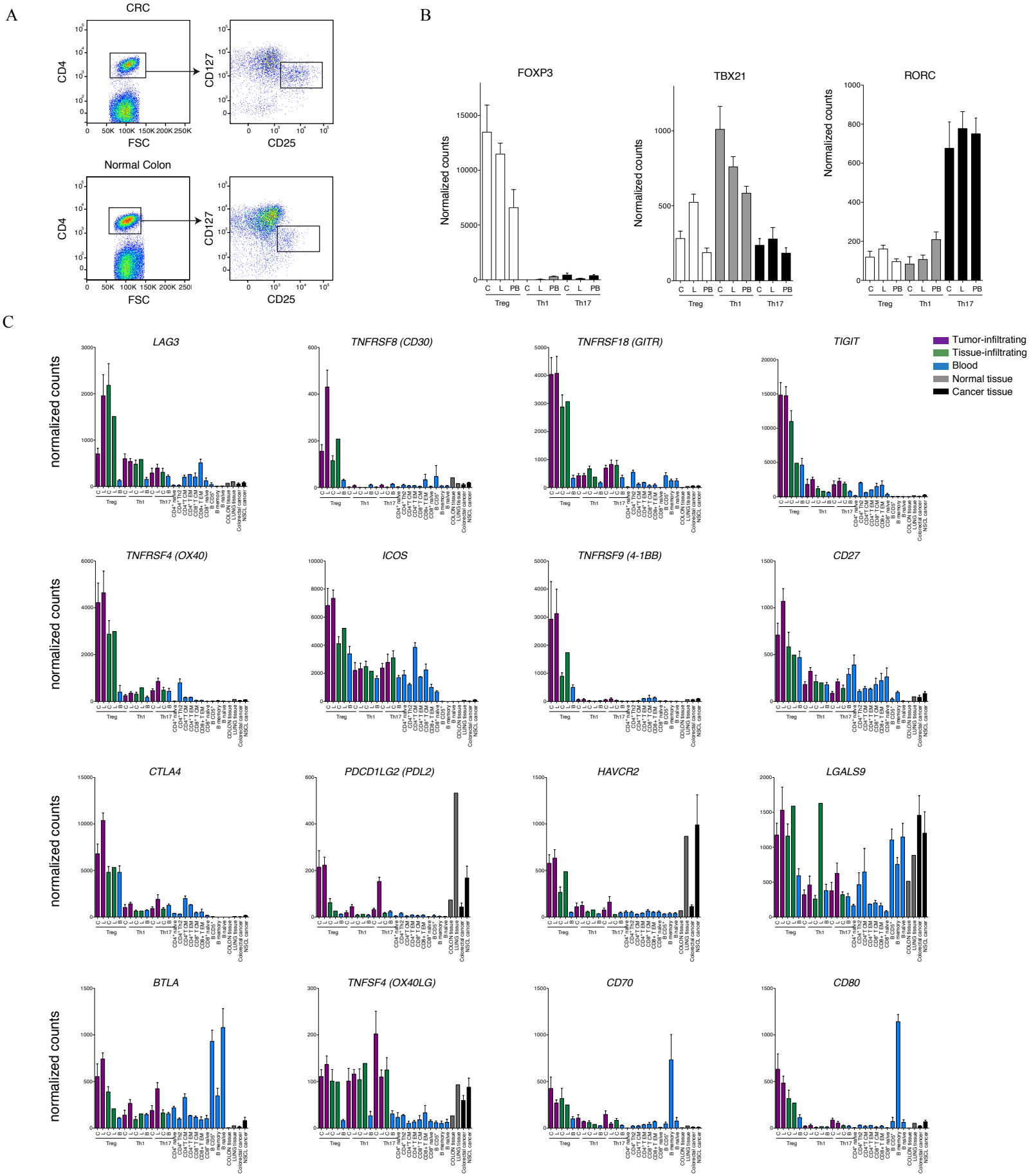

Figure S1 related to Figure 1. Transcriptome analysis of tumor infiltrating lymphocytes

(A) Representation of the sorting strategy of Treg cells infiltrating colorectal tumor or normal tissue.

(B) RNA-seq expression values (normalized counts) of FOXP3, TBX21 and RORC in CD4+ Th1, Th17 and Treg cells from CRC (C), NSCLC (L) or peripheral blood (PB) of healthy donors.

(C) RNA-seq normalized counts data for selected immune checkpoints and their ligands are shown as histogram plot. Cell population names are reported in the lower part of each graph, while gene names are shown in the upper part. To distinguish the origin of the different populations a color code has been assigned (upper right part of the figure).

Figure S2

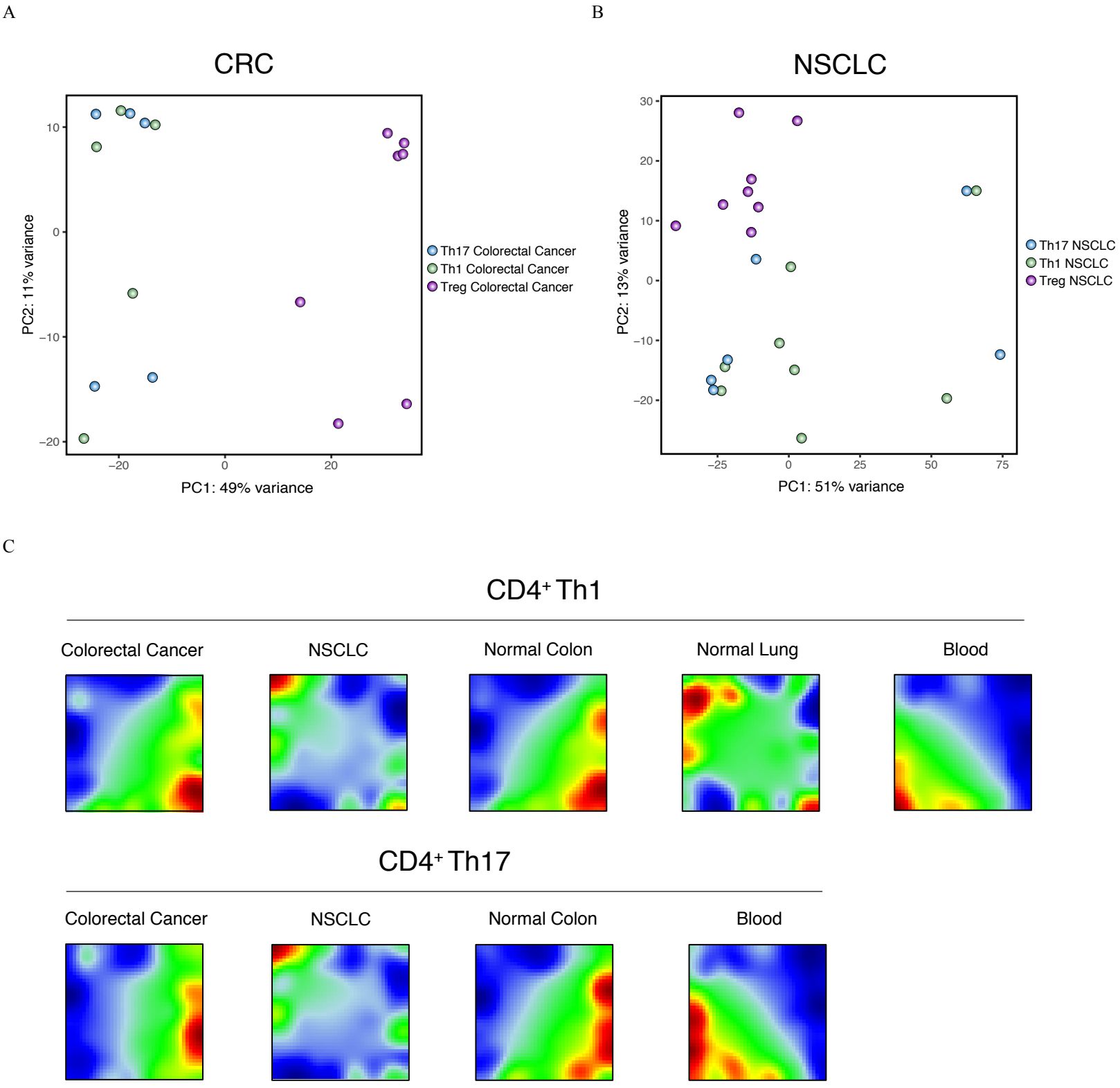

Figure S2 related to Figure 2. SOM analysis identifies co-regulated genes in tumor infiltrating Treg cells.
(A-B) Principal Component Analysis (PCA) has been performed on rlog-normalized (DESeq2) counts for tumor infiltrating CD4+ Treg, Th1 and Th17 cells RNA-seq data in CRC (A) and NSCLC (B) samples.
(C) Self-Organizing Maps analysis has been performed on the RNA-seq dataset comprising Th1and Th17 cell subsets. Bidimensional sample-level SOM profiles for different tissues are reported.

Figure S3

A

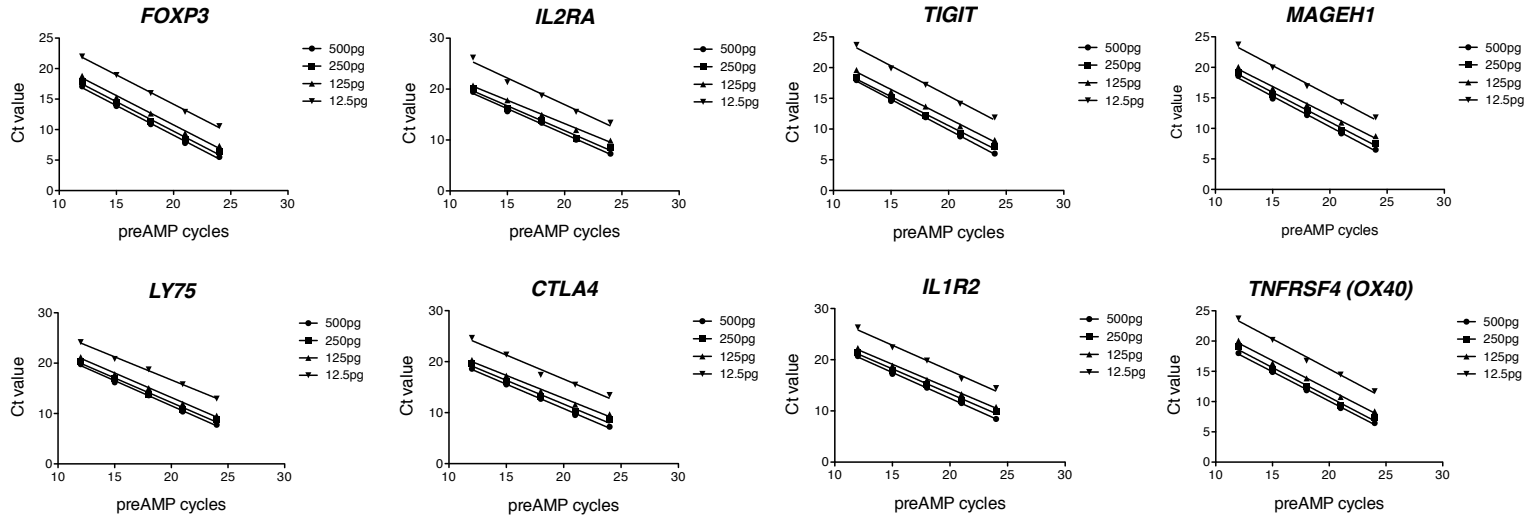

B

R^2	500pg	250pg	125pg	12.5pg
FOXP3	0.9967	0.9906	0.9933	0.9978
IL2RA	0.9951	0.9879	0.9966	0.9792
TIGIT	0.9987	0.9948	0.9949	0.992
MAGEH1	0.9965	0.9946	0.9941	0.9922
LY75	0.997	0.9917	0.997	0.9963
CTLA4	0.9977	0.9852	0.9918	0.9775
IL1R2	0.9987	0.993	0.9969	0.987
TNFRSF4 (OX40)	0.9982	0.9899	0.994	0.9925

C

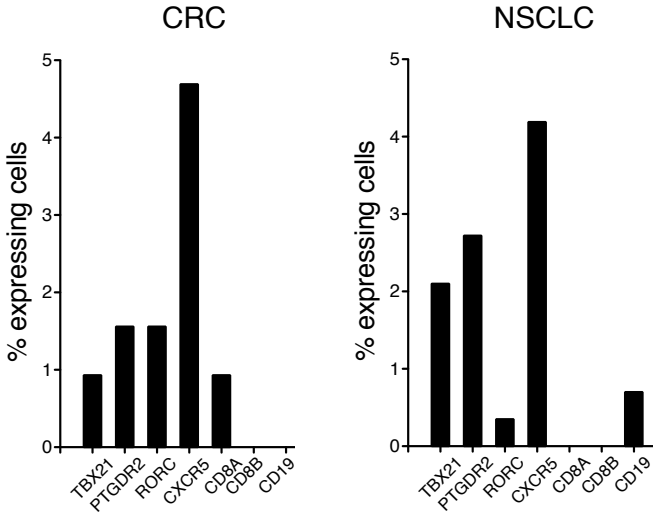

CELL TYPE	MARKERS
$CD4^+$ Th1	TBX21
$CD4^+$ Th2	PTGDR2
$CD4^+$ Th17	RORC
$CD4^+$ Tfh	CXCR5
$CD8^+$ cells	CD8A, CD8B
B cells	CD19

Figure S3 related to Figure 3. Single-cell analysis of tumor infiltrating Treg cells.

(A) Pre-amplification efficiency assessment. 500 pg, 250 pg, 125 pg or 12.5 pg of cDNA (total RNA equivalent), were pre-amplified for 12, 15, 18, 21 or 24 cycles and used as template in individual qPCRs for each gene. For each template condition Ct for each amount of pre-amplified cDNA (Y-axis) was plotted against the number of pre-amplification cycles performed (X-axis). A subset of 8 probes out of 79 is shown.

(B) Fitness of the linear correlation between amplification cycles and Ct values for each template condition was assessed and confirmed by R2.

(C) Assessment of CD4+ Treg, Th1, Th17, Th2, CD8+ T cells and B cell markers expression (percentage of expressing cells) in single Treg cells purified from NSCLC and CRC

Figure S4

A

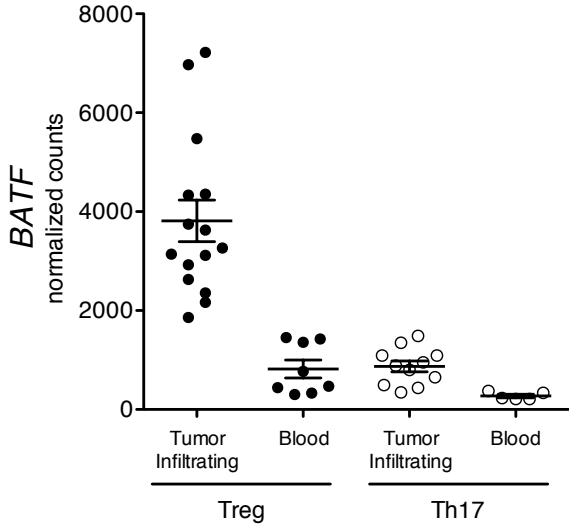

Figure S4 related to Figure 4. Comparison of BATF expression in CD4+ Treg vs Th17 cells.
BATF expression levels (RNA-seq normalized counts data) in CD4+ Treg and Th17 subsets isolated from tumor tissue or peripheral blood

Figure S5

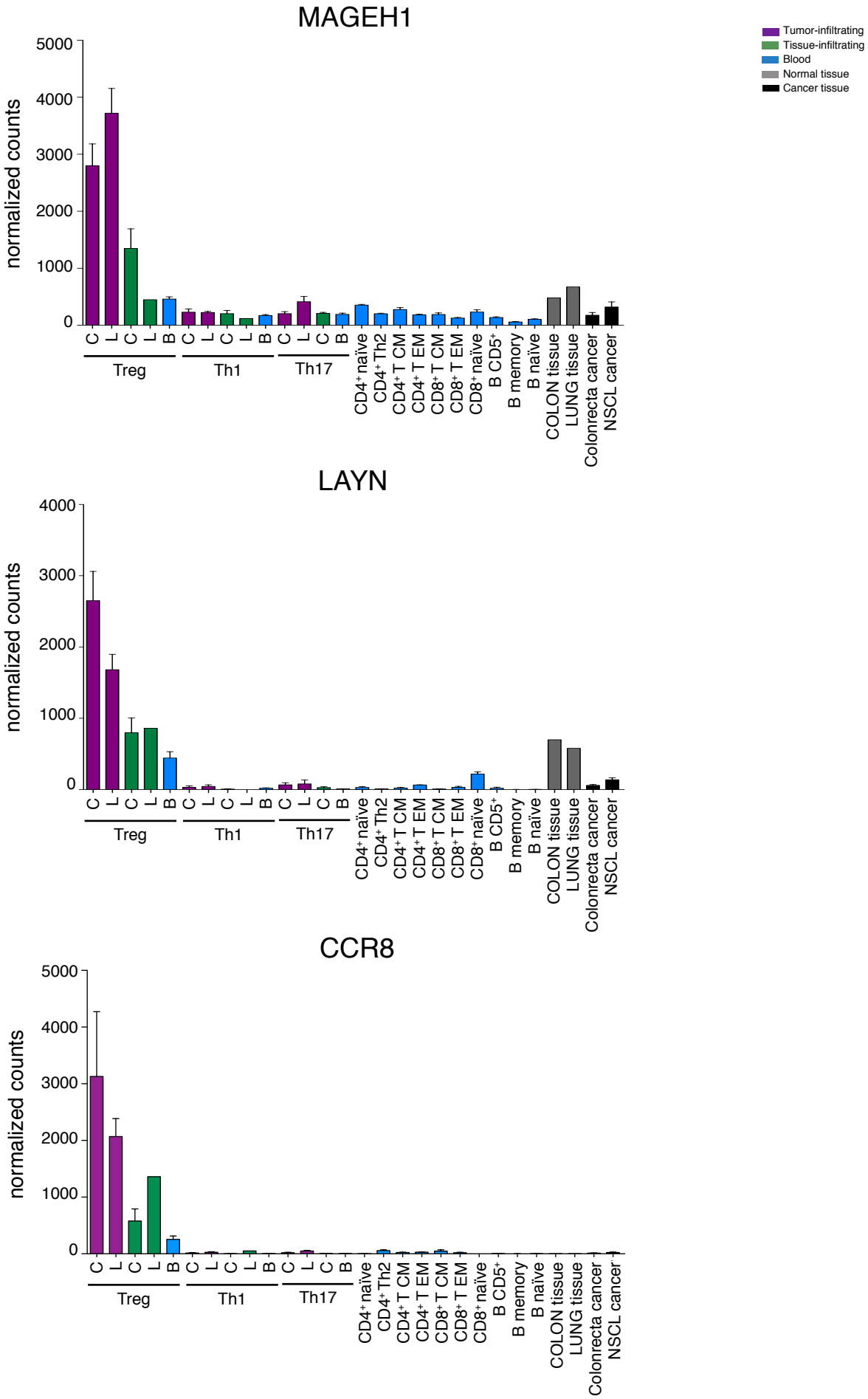

Figure S5 related to Figure 5. Expression levels of tumour-infiltrating Treg signature genes.
RNA-seq normalized counts data of three tumour-infiltrating Treg signature genes (MAGEH1, LAYN and CCR8) across listed cell populations. Cell populations are reported as a color code in the upper part of the figure.

SUPPLEMENTAL TABLES

Table S1 related to Table 1. Patients' information and histological analysis
For each cell subset profiled by RNA-sequencing, patient records are shown including: age at diagnosis, gender, smoking habit (for lung cancer patients), clinicopathological staging (TNM classification) tumor histotype and grade. For Treg cell isolated for qPCR experiment the same information are available, including also the number of live cells captured from each tumor and available for single-cell analysis. CRC: colorectal cancer; NSCLC: non-small cell lung cancer; (T): Tumor Sample; (H): Healthy Tissue; ADC: Adenocarcinoma; SCC: Squamous Cell Carcinoma; MUC ADC: Mucinous Adenocarcinoma.

Table S2 related to Figure 2. Co-regulated genes in tumor-infiltrating CD4+ Treg cells
A list of the co-regulated genes in tumor-infiltrating CD4+ Treg cells is reported.

Table S3 related to Figure 2. Tumor-infiltrating Treg cell Signature: GO enrichment
All the enriched GO terms (DAVID) for genes assigned to Treg cells regulated spots are reported with corresponding significance p-values.

Table S4 related to Figure 2. Expression levels of tumor-infiltrating Treg gene signatures in all the subsets analyzed
Normalized expression values of tumor-infiltrating Treg signature genes across listed cell populations. Cell populations are reported as a color code in the lower part of the table.

Table S5 related to Figure 1. Expression levels of immune checkpoints genes in all the subsets analyzed.
RNA-seq normalized counts data for selected immune checkpoints genes and their ligands in all the subsets analyzed. Color code for cell populations is reported in the lower part of the table.

Supplemental Table S6 Related to Figure 3.
List of TaqMan Probes and assay number used in RT-qPCR single-cell experiments

Taqman Assays Numbers			
Gene Name	Assay Number	Gene Name	Assay Number
BCL2L1	Hs00236329_m1	ACP5	Hs00356261_m1
EOS	Hs00223842_m1	BATF	Hs00232390_m1
AHCYL1	Hs00198312_m1	SLC35F2	Hs00213850_m1
NFE2L3	Hs00852569_g1	LAX1	Hs00214948_m1
IL12RB2	Hs00155486_m1	CCR8	Hs00174764_m1
CD177	Hs00360669_m1	ADPRH	Hs00153890_m1
OX40	Hs00937194_g1	IKZF2	Hs00212361_m1
METTL7A	Hs00204042_m1	CSF2RB	Hs00166144_m1
ENTPD1	Hs00969559_m1	NDFIP2	Hs00324851_m1
NFAT5	Hs00232437_m1	CADM1	Hs00942508_m1
CTSC	Hs00175188_m1	ICOS	Hs00359999_m1
SSH1	Hs00368014_m1	COL9A2	Hs00156712_m1
TMEM184C	Hs00217311_m1	LTA	Hs00236874_m1
HTATIP2	Hs01091727_m1	MAGEH1	Hs00371974_s1
HSDL2	Hs00953689_m1	IL21R	Hs00222310_m1
FOXP3	Hs01085834_m1	SSTR3	Hs01066399_m1
IL2RA	Hs00907778_m1	RNF145	Hs01099642_m1
LIMA1	Hs01035646_m1	LAPTM4B	Hs00363282_m1
NAB1	Hs00428619_m1	GRSF1	Hs00909877_m1
ACSL4	Hs00244871_m1	ANKRD10	Hs00214321_m1
ERI1	Hs00405251_m1	NPTN	Hs01033353_m1
FKBP1A	Hs00356621_g1	HS3ST3B1	Hs00797512_s1
LEPROT	Hs00956627_s1	TRAF3	Hs00936781_m1
NETO2	Hs00983152_m1	RRAGB	Hs01099767_m1
VDR	Hs00172113_m1	ZBTB38	Hs00257315_s1
CSF1	Hs00174164_m1	TIGIT	Hs00545087_m1
GITR	Hs00188346_m1	TFRC	Hs00951083_m1
IL1R2	Hs01030384_m1	JAK1	Hs01026983_m1
IL1R1	Hs00991010_m1	KSR1	Hs00300134_m1
LAYN	Hs00379511_m1	ZNF282	Hs00411965_m1
THADA	Hs00736554_m1	PTPRJ	Hs01119326_m1
CTLA4	Hs00175480_m1	CHRNA6	Hs02563509_s1
CHST2	Hs01921028_s1	IL2RB	Hs01081697_m1
CHST7	Hs00219871_m1	TBX21	Hs00203436_m1
LRBA	Hs01032231_m1	RORC	Hs01076112_m1
ETV7	Hs00903229_m1	CXCR5	Hs00540548_s1
LY75	Hs00982383_m1	CD8A	Hs00233520_m1
ADAT2	Hs00699339_m1	CD8B	Hs00174762_m1
GCNT1	Hs00155243_m1	PTGDR2	Hs00173717_m1
CASP1	Hs00354836_m1	CD19	Hs01047410_g1

SUPPLEMENTAL EXPERIMENTAL PROCEDURES

Human primary tissues

Primary human lung or colorectal tumors and non-neoplastic counterparts were obtained respectively from fifteen and fourteen patients who underwent surgery for therapeutic purposes at Fondazione IRCCS Ca' Granda, Policlinico or San Gerardo Hospitals (Italy). Records were available for all cases and included patients' age at diagnosis, gender, smoking habit (for lung cancer patients), clinicopathological staging (Sobin et al., 2009), tumor histotype and grade (Table S1). No patient received palliative surgery or neoadjuvant chemo- and/or radiotherapy. Informed consent was obtained from all patients, and the study was approved by the Institutional Review Board of the Fondazione IRCCS Ca' Granda (approval n. 30/2014).

Non-small-cell lung cancer (NSCLC) were cut into pieces and single-cell suspensions were prepared by using the Tumor Dissociation Kit, human and the gentleMACS™ Dissociator (Miltenyi Biotech cat. 130-095-929) according to the accompanying standard protocol. Cell suspensions were than isolated by ficoll-hypaque density-gradient centrifugation (Amersham Bioscience). Colorectal cancer (CRC) specimens were cut into pieces and incubated in DTT 0.1 mM (Sigma-Aldrich) for 10 min, then extensively washed in HBSS (Thermo Scientific) and incubated in 1 mM EDTA (Sigma-Aldrich) for 50 min at 37 °C in the presence of 5% CO2. They were then washed and incubated in type D collagenase solution 0.5 mg/mL (Roche Diagnostic) for 4 h at 37°C. Supernatants containing tumor infiltrating lymphocytes were filtered through 100 μm cell strainer, centrifuged and fractionated 1800X g for 30 min at 4°C on a four-step gradient consisting of 100%, 60%, and 40% and 30% Percoll solutions (Pharmacia). The T cell fraction was recovered from the inter- face between the 60% and 40% Percoll layers.

CD4 T cell subsets were purified by FACS sorting using the following fluorochrome conjugated antibodies: anti-CD4 APC/Cy7 (Biolegend clone OKT4), anti-CD27 Pacific Blue (Biolegend, clone M-T271), anti-IL7R PE (Milteniy, clone MB15-18C9), anti-CD25 PE/Cy7 (eBioscience, clone BC96), anti-CXCR3 PE/Cy5 (BD, clone 1C6/CXCR3), anti-CCR6 APC (Biolegend, clone G034E3) and anti-CCR5 FITC (Biolegend, clone j418F1) using a FACSAria II (BD).

Flow cytometry

To validate surface marker expression cells were directly stained with the following fluorochrome-conjugated antibodies and analyzed by flow cytometry: anti-CD4 (Biolegend, clone OKT4); anti-PD-L2 (Biolegend, Clone CL24F.10C12); anti-CD127 (eBioscience, clone RDR5); anti-BATF (eBioscience, clone MBM7C7), anti-GITR (eBioscience, clone eBIOAITR), anti-CD25 (Miltenyi, clone 4E3) and anti 4-1BB (eBioscience clone 4B4) anti CCR8(Biolegend clone L263G8) anti CD30 (eBioscience, clone Ber-H2) anti PD-L1 (Biolegend clone 29E.2A3) anti TIGIT (eBioscience, clone MBSA43) anti IL1R2 (R and D clone 34141) IL21R (Biolegend clone 2G1-K12) anti OX40 (Biolegend clone Ber-ACT35). Intracellular staining was performed using eBioscience Foxp3 staining kit according to the manufactured's protocol (eBioscience cat 00-5523-00). Briefly cells were harvested and fixed for 30 min in fixation/permeabilization buffer at 4 °C, and than stained with anti-FOXP3 antibody (eBioscience, clone 236A/E7) and anti-BATF (ebioscience clone MBM7C7) in permeabilisation buffer for 30 min at 4 °C. Cells were then washed two times, resuspended in FACS washing buffer and analyzed by flow cytometry.

Suppression assay.

4×10^4 carboxyfluorescein diacetate succinimidyl ester (CFSE)-labeled (1 μM) responders $Naive^+$ T cells from healthy donors were cocultured with different E/T ratio with unlabeled $CD127^-CD25^{low}CD4^+$ T cells sorted from TILs or PBMCs of patients with CRC or NSCLC, using FACS Aria II (BD Biosciences) , in the presence of $CD11c^+CD1c^+$dentritic cells as antigen-presenting cells and 0.5 mg/ml anti-CD3 (OKT3) mAb. Proliferation of CFSE-labeled cells was assessed by flow cytometry after 96 hr culture.

Competition assays with blocking antibodies were performed following the same protocol starting from $2x10^5$ CFSE labeled CD4+ naïve T cells from healthy donors cocultured at 1:32 Responders/Tumor Treg cell ratio. The following antibodies at a final concentration of 20μg/ml were used purified anti-human PDL-1 (biolegend clone 29E.2 A 3); purified anti-human PD-L2 (biolegend clone MIH18); anti-human Functional Grade (ebioscience clone MBSA43)

RNA isolation and RNA sequencing

RNA from tumor-infiltrating lymphocytes was isolated using mirVana Isolation Kit. Residual contaminating genomic DNA was removed from the total RNA fraction using Turbo DNA-free (Thermo Fisher). The RNA yields were quantified using the QuantiFluor RNA System (Promega) and the RNA quality was assessed by the Agilent 2100 Bioanalyzer (Agilent). Libraries for Illumina sequencing were constructed from 50 ng of

total RNA with the Illumina TruSeq RNA Sample Preparation Kit v2 (Set A). The generated libraries were loaded on to the cBot (Illumina) for clustering on a HiSeq Flow Cell v3. The flow cell was then sequenced using a HiSeq 2500 in High Output mode (Illumina). A paired-end (2×125) run was performed.

RNA-seq data analysis
Raw .fastq files were analyzed using FastQC v0.11.3, and adapter removal was performed using cutadapt 1.8. Cutadapt is run both for reverse and forward sequences with default parameters [--anywhere <adapter1> --anywhere <adapter2> --overlap 10 --times 2 --mask-adapter]. Adapter sequences used for libraries preparation are

Adapter1:
AGATCGGAAGAGCACACGTCTGAACTCCAGTCACNNNNNNATCTCGTATGCCGTCTTCTGCTTG

Adapter2:
AGATCGGAAGAGCGTCGTGTAGGGAAAGAGTGTAGATCTCGGTGGTCGCCGTATCATT

Trimming was performed on raw reads using Trimmomatic (Bolger et al., 2014): standard parameters for phred33 encoding were used: ILLUMINACLIP (LEADING:3 TRAILING:3 SLIDINGWINDOW:4:15), MINLEN parameter was set to 50.

Mapping and quantification: reads mapping to the reference genome (GRCh38) was performed on quality-checked and trimmed reads using STAR 2.4.1c: [STAR --genomeDir <index_star> --runThreadN <cpu_number> --readFilesIn <trimmed>_R1.fastq.gz <trimmed>_R2_P.fastq.gz --readFilesCommand zcat]. The reference annotation is Ensembl v80. The overlap of reads with annotation features found in the reference .gtf was calculated using HT-seq v0.6.1. The output computed for each sample (raw read counts) was then used as input for DESeq2 analysis. Raw counts were normalized using DESeq2's function 'rlog', and normalized counts were used to perform and visualize Principal Component Analysis (PCA) results (using DESeq2's 'plotPCA' function).

Differential expression analysis: differential expression analyses of tumor-infiltrating CD4+ Treg/Th1/Th17 subsets vs. CD4+ Treg/Th1/Th17 from PBMC were performed using DESeq2. Upregulated/downregulated genes were selected for subsequent analyses if their expression values were found to exceed the threshold of 0.05 FDR (Benjamini-Hochberg correction).

SOM (theory): SOMs can be thought of as a spatially constrained form of k-means clustering (Ripley, 1996). In this analogy, every unit in the grid corresponds to a cluster to which a certain number of gene expression input vectors are mapped. For each vector during the training phase of the algorithm, the "winning unit" (the one most similar to the current training object) will be updated to become even more similar. A weighted average is used, where the weight of the new object is one of the training parameters of the SOM. The update is not restricted to the winning unit, but it is extended to the units in the immediate neighborhood, so that the structure itself of the map can fit the data. The size of the neighborhood progressively shrinks, so that eventually only the winning units are adapted. In the oposSOM package (Loffler-Wirth et al., 2015), a rectangular SOM topology with a Gaussian neighborhood function is used. Upon training completion, the distance of vectors describing groups of samples (e.g. tumor-infiltrating lymphocytes) is calculated (using the same metric that was used for training) and a map with color-coded distances that is specific for the considered condition is drawn. These expression portraits exhibit characteristic spatial color patterns and serves as fingerprint of the transcriptional activity.

SOM analysis: In order to translate RNA-seq expression data into metadata of reduced dimensions and identify genes that are preferentially expressed in tumor-infiltrating lymphocyte subsets, Self-Organizing Maps (SOMs) analysis was performed on our dataset. This method transformed the whole genome expression pattern of about 7,000 differentially expressed genes into a SOM coordinate system, which allowed for intuitive visualization of transcriptional activity of each sample in terms of mosaic portraits. SOM analysis combines strong clustering, dimensionality reduction, multidimensional scaling and visualization capabilities which have been shown to be advantageous compared to alternative methods such as clustering heatmaps and negative matrix factorization when applied to molecular high-throughput data (Wirth et al., 2012). SOM maps constitute fingerprints of the transcriptional activity of the respective cell population sample and allow for direct comparison of the expression of individual samples in a simple and intuitive way. The color gradient is instrumental to visualize over- or underexpression of the nodes for the particular sample compared with the mean expression level of each node in the pool of all samples

studied.Analyses were carried out using the R package oposSOM (Loffler-Wirth et al., 2015) using default parameters. Expression values of genes selected in the previous differential expression step were Z-score normalized and supplied in input to the automated pipeline for SOM training and analysis. Genes from up/downregulated spots in the bidimensional output space were selected according to FDR threshold (<0.1) at group-level. Expression values of genes assigned to regulated spots extracted from the oposSOM output were then subject to correlation analysis using model vectors to further refine the results and genes having expression profiles with P-val<0.05 were discarded from further analysis and signature definition.

Pearson correlation analyses: correlation analyses were performed using Pearson correlation metric, and significance p-values were calculated using the *cor.test* function from the WGCNA R package.

GO analysis: a GO enrichment analysis was performed for biological process terms associated with genes assigned to up/downregulated spots in the SOM bidimensional space using DAVID (Huang da et al., 2009). Adjusted p-val has been used for terms ranking and selection (<0.05).

Capturing of single cells, preparation of cDNA and single-cell PCR
Treg cells from 5 CRC and 5 NSCLC specimens were isolated as previously described (See also Table S1).Single cells were captured on a microfluidic chip on the C1 System (Fluidigm) and whole-transcriptome amplified. cDNA was prepared on chip using the SMARTer Ultra Low RNA kit (Clontech). Cells were loaded onto the chip at a concentration of 3–5E5 cells/ml, stained for viability (LIVE/DEAD cell viability assay; Thermo Fisher) and imaged by phase-contrast and fluorescence microscopy to assess the number and viability of cells per capture site. Only single, live cells were included in the analysis. For qPCR experiments, harvested cDNA was pre-amplified using a 0.2X pool of primers prepared from the same gene expression assays to be used for qPCR. Pre-amplification allows for multiplex sequence-specific amplification 78 targets. In detail, a 1.25 µl aliquot of single cell cDNA was pre-amplified in a final volume of 5 µl using 1 µl of PreAmp Master Mix (Fluidigm) and 1.25 µl pooled TaqMan assay mix (0.2x). cDNA went through amplification by denaturing at 95°C for 15 s, and annealing and amplification at 60°C for 4 min for 20 cycles.After cycling, pre-amplified cDNA was diluted 1:5 by adding 20 µl TE Buffer to the final 5 µl reaction volume for a total volume of 25 µl.
Single-cell gene expression experiments were performed using the 96x96 quantitative PCR (qPCR) DynamicArray microfluidic chips (Fluidigm). A 2.25 µl aliquot of amplified cDNA was mixed with 2.5 µl of TaqMan Fast Adavanced Master Mix (Thermo Fisher) and 0.25 µl of Fluidigm's "sample loading agent," then inserted into one of the chip "sample" inlets. A 2.5 µl aliquot of each 20X TaqMan assay was mixed with 2.5 µl of Fluidigm's "assay loading agent" and individually inserted into one of the chip "assay" inlets. Samples and probes were loaded into 96 x96 chips using an IFC Controller HX (Fluidigm), then transferred to a BioMark real-time PCR reader (Fluidigm) following manufacturer's instructions. A list of the 78 TaqMan assays used in this study is provided below.

Single-cell data analysis: The Quality Threshold in the BioMark™ Analysis software is a qualitative tool designed to measure the "quality" of each amplification curve. Basically, each amplification curve is compared to an ideal exponential curve and as the quality score approaches 1 the closer it is to ideal. The further the curve is from ideal, its quality score approaches 0. The default cutoff of 0.65 is an arbitrary value set by Fluidigm. Any curve above 0.65 passes. Any curve below, fails. Baseline correction was set on Linear (Derivative)[default]. Ct Threshold Method was set on Auto (Detectors). This method independently calculates a threshold for each detector on a chip. For clustering and downstream analysis, raw Cts have been converted to Log2Exp by using a Limit of Detection (LOD) of 35, which corresponds to the last PCR cycle. Co-expression analysis has been performed by considering both CRC and NSCLC samples on those genes for which both FOXP3 and IL2RA were co-expressed at least to 2%. Gene's levels above the background were depicted as violin plots after log2 scale transformation by ggplot2 (v. 2.1.10). The violin color gradient is the percentage of cells that are expressing the gene of interest and the upper bound of the color scale is the maximum percentage of cells that express a gene of the whole geneset.

Procedure for the removal of transcripts whose expression values are affected by the 'dropout' effect.
Single-cell qPCR data are inherently noisy, and due the limitations of current technologies the expression patterns of a certain number of genes may be afftected by the 'dropout effect'. We performed a gene selection procedure in order to take into account this 'dropout' effect and discard those genes whose expression values cannot be reliably used in a binary comparison (tumor-peripheral vs blood). We fitted a number of parametric distributions to the ratios of detected genes on the total number of tumor cells (both NSCLC and CRC) and selected the reciprocal inverse Gaussian continuous random variable as best fit. We then calculated the median value of the fitted distribution and discarded those genes whose

detection ratio is less than this threshold value (at least 8.4% of detection). We reasoned that these genes are more likely to be affected by the 'dropout' effect. With this threshold we selected 45 genes for which a non-parametric T-test (Wilcoxon Mann Whitney test $p<0.05$) has been performed (by comparing tumor vs. peripheral blood samples)

Meta analysis Kaplan-Meier and stage correlation

Statistical analysis was performed by using the R survival package (Therneau T. 2013). Survival times were calculated as the number of days from initial pathological diagnosis to death, or the number of days from initial pathological diagnosis to the last time the patient was reported to be alive. The Kaplan-Meier (KM) was used to compare the high and low expression levels of the tumor-Treg cell signature transcripts in either CRC (GSE17536) and NSCLC (GSE41271) patients. For both studies annotation was normalized to four tumor stages (1,2,3,4). For study GSE41271 five patients were excluded due to incomplete or inaccurate annotation (GSM1012883,GSM1012884,GSM1012885,GSM1013100,GSM1012888), retaining a total of two hundred and sixty three patients. Patients from both studies were labeled as 'High' 'Low' whether or not their relative expression values exceeded a decision boundary (mean of the samples). We define $\ddot{x}_{ij}$ to denote the relative expression of the gene *i* for the *n* samples of the study normalized to the CD3 level:

$$\ddot{x}_{i,j} = \frac{x_{i,j}}{x_{CD3G,j}}\ ; \qquad i = (CCR8, MAGEH1, LAYN) \quad j = 1,2,\ldots\ldots n\ samples$$

To classify a patient, a threshold on the $\ddot{x}_{ij}$ is required and defined as

$$T_{(Upper,Lower)} = median(\ddot{x}_{i,j}) \pm \frac{\sigma(\ddot{x}_{i,j})}{10}$$

where $T_{(Upper,Lower)}$ represent the upper and lower extreme of the decision boundary:

$$\begin{cases} \ddot{x}_{i,j} > T_{Upper}\ High \\ \ddot{x}_{i,j} < T_{Lower}\ Low \\ T_{Upper} \leq \ddot{x}_{i,j} \leq T_{Lower}\ excluded \end{cases}$$

We examined the prognostic significance of tumor Treg cells transcripts by using log-rank statistics; a p-value of less than 0.05 was considered statistically significant.

Since the log-rank test resulted in a p-value of less than 0.05, a post stage comparison by means of box plot representation was performed in order to evaluate the correlation degree between the expression level of the transcripts and tumor stages in the cohort of CRC patients. . The annotation was normalized to four tumor stages (1,2,3,4).

SUPPLEMENTAL REFERENCES

Bolger, A.M., Lohse, M., and Usadel, B. (2014). Trimmomatic: a flexible trimmer for Illumina sequence data. Bioinformatics *30*, 2114-2120.

Huang da, W., Sherman, B.T., and Lempicki, R.A. (2009). Systematic and integrative analysis of large gene lists using DAVID bioinformatics resources. Nat Protoc *4*, 44-57.

Loffler-Wirth, H., Kalcher, M., and Binder, H. (2015). oposSOM: R-package for high-dimensional portraying of genome-wide expression landscapes on bioconductor. Bioinformatics *31*, 3225-3227.

Ripley, B. D. (1996) Pattern Recognition and Neural Networks. Cambridge: Cambridge University Press. [i, 2, 8, 36, 42, 59, 69, 73, 79, 91, 92]

Sobin, L.H., Gospodarowicz, M.K., Wittekind, C., International Union against Cancer., and ebrary Inc. (2009). TNM classification of malignant tumours (Chichester, West Sussex, UK ; Hoboken, NJ: Wiley-Blackwell,), pp. xx, 310 p.

Therneau T. 2013. *A package for survival analysis in S.* R package version 2.37-4.

Wirth, H., von Bergen, M., and Binder, H. (2012). Mining SOM expression portraits: feature selection and integrating concepts of molecular function. BioData Min *5*, 18.